Bieser, J.; De Simone, F.; Gencarelli, C.; Geyer, B.; Hedgecock, I.;
Matthias, V.; Travnikov, O.; Weigelt, A.:

A diagnostic evaluation of modeled mercury wet depositions in Europe using atmospheric speciated high-resolution observations

In: Environmental Science and Pollution Research (2014) Springer

DOI: 10.1007/s11356-014-2863-2

A diagnostic evaluation of modelled mercury wet depositions in Europe using atmospheric speciated high resolution observations.

Bieser, J.[1,*], De Simone, F.[2], Gencarelli, C.[2], Geyer, B.[1], Hedgecock, I.[2], Matthias, V.[1], Travnikov, O.,[3] Weigelt, A.[1]

[1] Helmholtz-Zentrum Geesthacht, Institute of Coastal Research, Max-Planck-Str. 1, 21502 Geesthacht, Germany

[2] CNR - Istituto Inquinamento Atmosferico, U.O.S. di Rende, c/o: UNICAL-Polifunzionale, 87036 Rende, Italia

[3] Meteorological Synthesizing Center-East of EMEP, 2nd Roshchinsky proezd., 8/5, Moscow 115419, Russia

Abstract

This study is part of the Global Mercury Observation System (GMOS), a European FP7 project dedicated to the improvement and validation of mercury models to assist in establishing a global monitoring network and to support political decisions. One key question about the global mercury cycle is the efficiency of its removal out of the atmosphere into other environmental compartments. So far, the evaluation of modelled wet deposition of mercury was difficult because of a lack of long term measurements of oxidized and elemental mercury. The oxidized mercury species GOM (Gaseous Oxidized Mercury) and PBM (Particle Bound Mercury) which are found in the atmosphere in typical concentrations of a few to a few tens pg/m³ are the relevant components for the wet deposition of mercury.

In this study, the first European long-term dataset of speciated mercury taken at Waldhof/Germany was used to evaluate deposition fields modelled with the chemistry transport model (CTM) CMAQ and to analyse the influence of the governing parameters. The influence of the parameters precipitation and atmospheric concentration was evaluated using different input datasets for a variety of CMAQ simulations for the year 2009. It was found, that on the basis of daily and weekly measurement data the bias of modelled depositions could be explained by the bias of precipitation fields and atmospheric concentrations of GOM and PBM. A correction of the modelled wet deposition using observed daily precipitation increased the correlation, on average, from 0.17 to 0.78. An additional correction based on the daily average GOM and PBM concentration lead to a 50% decrease of the model error for all CMAQ scenarios. Monthly deposition measurements were found to have a too low temporal resolution to adequately analyse model deficiencies in wet deposition processes due to the non-linear nature of the scavenging process. Moreover, the general overestimation of atmospheric GOM by the CTM in combination with an underestimation of low precipitation events in the meteorological models lead to a good agreement of total annual wet deposition besides the large error in weekly deposition estimates.

Moreover, it was found that the current speciation profiles for GOM emissions are the main factor for the overestimation of atmospheric GOM concentrations and might need to be revised in the future. The assumption of zero emissions of GOM lead to an improvement of the mean normalized bias for three-hourly observations of atmospheric GOM from 9.7 to 0.5, Furthermore, the diurnal correlation between model and observation increased from 0.01 to 0.64. This is a strong indicator, that GOM is not directly emitted from primary sources but is mainly created by oxidation of GEM.

1. Introduction

Mercury is a global pollutant that is known to have adverse effects on human health (UNEP 2002; 2013a). Because of anthropogenic emissions from fossil fuel burning the amount of mercury available in the environment is steadily increasing. Recent studies have shown that the atmospheric mercury burden has tripled since pre-industrial times (UNEP 2008; Amos et al. 2012).

Due to its severity, the problem of global mercury pollution is in the focus of several international conventions such as the UNEP mercury program (UNEP, 2013b) and the UN-ECE Long-Range Transport of Atmospheric Pollution Convention-Task Force on Hemispheric Transport of Air pollution (HTAP) (ECE, 2010). Major scientific questions about atmospheric mercury are the oxidization processes of elemental mercury, global and regional transport patterns, and a better

understanding of mercury emissions.

In the atmosphere mercury exists in three forms: Gaseous Elemental Mercury (GEM), Gaseous Oxidized Mercury (GOM), and Particle Bound Mercury (PBM). For the atmospheric long range transport GEM is the most important substance. This is due to the long life time of the species and the fact that it represents the largest fraction (99%) of the total atmospheric mercury (Gay et al., 2013; Weigelt et al., 2013). However, an extremely important question in order to understand the global mercury cycle is the deposition of mercury from the atmosphere. A recent study by Zhang et al. (2012b) found that between 50 and 70% of the total mercury deposition is due to GOM and PBM, although these species make up only 1% of the total gaseous mercury (TGM). GEM plays only a role for dry deposition and it needs to be considered that depending on the surface type about half of the deposited GEM is quickly re-emitted into the atmosphere (Zhang et al, 2012a). On annual average water bodies and soils can even release more GEM than is deposited, depending on deposition in the past (Bash, 2010). In Europe for example, the Mediterranean, Baltic, and North Sea have been identified as large sources of GEM (Kuss and Schneider, 2007; Strode et al., 2007; Zager et al., 2007). Therefore, to quantify the input of mercury into different ecosystems it is very important that CTMs are able to calculate the atmospheric concentration as well as the deposition of these species. However, due to the very low concentrations of GOM and PBM (1-100 pg/m³) until recently no continuous measurements for these species were available. This lack of observational data is now being addressed by the Global Mercury Observation System (GMOS). The European FP7 project focuses on the improvement and validation of mercury models to assist establishing a global monitoring network and to support political decisions. Recently, Weigelt et al. (2013) published the first full-speciation long-term measurement series for atmospheric mercury in Europe.

Over the last decade a variety of global CTMs were upgraded to model mercury in the atmosphere. Eventually, these efforts led to a large inter-comparison study of atmospheric mercury models (Ryaboshapko et al. 2005, 2007a, 2007b) as well as regional scale mercury model inter-comparisons (Bullock et al. 2008). These studies mainly focused on operational evaluations for the investigation of model uncertainties as well as diagnostic evaluations of model parameterizations. Concerning deposition, one result of these inter-comparisons is that a comprehensive evaluation of atmospheric mercury models is hindered by the lack of observational data for speciated mercury (Bullock et al. 2009). Generally, the utilized CTMs were able to reproduce the observed annual mercury wet depositions (Baker and Bash, 2012). However, Zhang et al. (2012b) found that deposition patterns predicted by models, which indicated higher depositions near major sources, were not in agreement with observations.

In this study, which is part of the GMOS project, we used the mercury version of the Community Multiscale Air Quality (CMAQ) model to calculate mercury concentrations and depositions over Europe. CMAQ is a CTM that was originally developed by the U.S. EPA to evaluate air pollution by ozone and particulate matter (PM) (Byun and Ching, 1999). In 2001 CMAQ was extended to simulate the atmospheric pathway of GEM, GOM, and PBM. Bullock and Brehme (2002) evaluated the performance of CMAQ-Hg by comparison of modelled and observed wet deposition fluxes in the eastern United States.

Using the newly available high resolution measurements of GEM, GOM, PBM, and wet deposition for Europe we analyse the capability of the CMAQ-Hg model to reproduce observations and determine the influence of different processes on model biases. It is of course impossible to evaluate a model for entire Europe using a single observation site. Nonetheless, the combined measurement of speciated mercury concentrations and mercury wet deposition allows to evaluate the deposition parameterization of the model and to analyse potential uncertainties in the CTM parameterizations and input datasets. The main focus of this diagnostic evaluation are the different sources for GOM and PBM in the model such as the primary emissions and the oxidation of GEM.

2. Methodology

For this study atmospheric mercury concentrations and mercury depositions over Europe were investigated with an air quality modelling system. The year 2009 was chosen because of the availability of high resolution mercury observations for this particular year (Weigelt et al., 2013). To determine the influence of different parameters on the modelled mercury deposition a diagnostic evaluation was performed (Dennis et al., 2010). For this, the CTM was run using different input datasets based on different models and parameterizations. In the following the models and datasets employed for this study are introduced.

2.1 Chemistry Transport Model (CMAQ-Hg)

CMAQ-Hg was set up on a Lambert Conformal equal area domain over Europe with a resolution of 72x72km². The rather low resolution for a regional model was chosen in order to allow for several annual CTM runs to be performed. Moreover, the resolution is suitable for the available measurement data for speciated mercury. Assuming average wind speeds below 10 m/s for the model domain and measurements, which have a temporal resolution of 3 hours. In order to test the influence of the model resolution a short episode was calculated on a domain with 24x24km² grid size. On the vertical dimension, CMAQ-Hg was set up with 30 layers based on sigma pressure levels. The CMAQ version used for this study is the newest release version 5.0.1 compiled with the multi pollutant version of carbon-bond 5 photochemical mechanism with updated chlorine and toluene chemistry (cb05tump) with on-line photolysis and the aero6 aerosol module.

CMAQ-Hg includes five gas phase reactions for the oxidation of mercury with ozone (1), hydroxy radicals (2,3) and chlorine (4,5). Reactions with bromine are not considered by the CMAQ-Hg mercury mechanism. In the model, the dominant reaction over northern Europe is the oxidation by ozone (1). Generally 50% of the products are allocated to GOM and 50% to PBM (Bullock and Brehme, 2002). This ratio is important because the effectiveness of deposition differs between these species. For the H_2O_2 and Cl_2 reactions GOM is the only product. The exact process of mercury oxidation, concerning both the oxidant and the product ratios, is still unknown and subject to scientific research. For this study the standard CMAQ mercury mechanism was used, which is similar to mechanisms used by other global and regional models (e.g. ECHMERIT, GLEMOS) (Jung et al., 2009; Travnikov and Ilyin, 2009). To evaluate the influence of the chemical reactions, we tested a modified version of CMAQ-Hg where all reactions produce GOM only. The assumption behind this modification is, that the gas phase chemistry can only produce gaseous products and that particulate mercury is only formed after oxidation of GEM.

$$HG + O_3 \rightarrow 0.5\ PBM + 0.5\ GOM \quad (1)$$

$$HG + OH \rightarrow 0.5\ PBM + 0.5\ GOM \quad (2)$$

$$HG + H_2O_2 \rightarrow GOM \quad (3)$$

$$HG + CL2 \rightarrow GOM \quad (4)$$

$$HG + CL + M \rightarrow 0.5\ HG + 0.5\ GOM + M \quad (5)$$

A basic CMAQ run without mercury chemistry has been evaluated concerning criteria pollutants (Bieser et al., 2011) and particles (Matthias et al., 2008). This is of particular interest because of the importance of ozone for the oxidation of GEM (1) at Waldhof. A comparison with hourly ozone measurements at 40 EMEP stations has shown that 80% of the simulated concentrations were within a factor of 2 of observations. Generally, CMAQ underestimated ozone depletion during night time leading to an average fractional bias of 0.3 (Bieser et al., 2011).

2.2 Emissions

The emission data for criteria pollutant precursors were created with the SMOKE for Europe (SMOKE-EU) emission model (Bieser et al., 2011) which is based on the U.S. EPA emission model SMOKE (Houyoux et al., 2000; UNC, 2005). The emission dataset includes anthropogenic and biogenic emissions of CO, NOx, SO_2, NH3, VOC, PM_{10}, and $PM_{2.5}$. The VOC emissions were speciated according to the cb05 photochemical mechanism (Yarwood et al., 2005; Passant, 2002). $PM_{2.5}$ emissions were speciated according to the areo6 CMAQ aerosol module using sectoral emission factors of the SPECIATE4.0 database. Finally, speciated mercury emissions from the Arctic Monitoring and Assessment Programme (AMAP) emission inventory were added to the dataset (Pacyna et al. 2006). AMAP provides gridded annual total mercury emissions on a 0.5x0.5° global domain. These gridded annual total mercury emissions were temporally disaggregated with SMOKE-EU. The effective emission height of industrial mercury emissions from stacks was based on plume rise calculations (Bieser et al., 2012).

The partitioning of mercury emissions for power plants provided by AMAP suggests that 40% of the total mercury is emitted as GOM, 10% as PBM, and 50% as GEM. As a result, a large amount of oxidized mercury is directly introduced into the model domain by emissions compared to the oxidization in the atmosphere by the chemistry mechanism as described in equations (1) to (5). Recent air-born measurements inside the plume of a major coal fired power plant have indicated that less than 1% of the total mercury emissions are in the form of GOM (Weigelt, p.c.). One reason for this could be the in plume reduction of oxidized mercury (Lohmann et al., 2006; Vijayaraghavan et al., 2008). In order to evaluate the influence of primary mercury emissions additional emission scenarios without any primary oxidized mercury emissions were created as input for CMAQ-Hg.

2.3 Meteorological fields

Mercury deposition depends strongly on the meteorological conditions, in particular on the precipitation fields. Two alternative sets of meteorological input fields were used. The first one was calculated with the COSMO-CLM (CCLM) meteorological model, which is the standard input for CMAQ-Hg at HZG (Rockel et al., 2008). CCLM was run on a 0.22x0.22° domain and driven with reanalysis data from NCEP. The exact model setup of CCLM is documented in Rockel and Geyer (2008).

The second dataset was created with the Weather Research and Forecasting model (WRF) (Michalakes et al., 2004; Skamarock et al. 2008). For this study WRF was run using the Purdue-Lin microphysics processes and the Mellor-Yamada-Janjic (MYJ) scheme for Planetary Boundary Layer parameterization. The MYJ scheme describes vertical fluxes due to eddy transport while the horizontal eddy diffusivity is calculated with a Smagorinsky 1st order closure. The surface layer parametrisation employed was the Eta surface layer scheme whit Noah Land Surface Model. For longwave and shortwave radiation we used respectively Rapid Radiative Transfer Model (RRTM) and Dudhia scheme, while for cumulus parametrisation we used the Kain-Fritsch scheme. Meteorological initial and boundary condition are obtained from the NCEP global final analysis from the Global Forecast System (grid resolution of 1° by 1° at six hourly intervals).

2.4 Boundary conditions

Boundary conditions for mercury and all criteria pollutant precursors were taken from the global CTM ECHMERIT (Jung et al. 2009) which is based on the fifth generation Atmospheric General Circulation Model ECHAM5 (Roeckner et al. 2003, 2006). ECHMERIT includes a gas phase chemistry module derived from the CBM-Z mechanism (Zaveri et al. 1999), and an aqueous phase chemistry module based on the MECCA model (Sander et al. 2005). In addition, ECHMERIT models four mercury species: elemental mercury (Hg0), gaseous oxidised Hg (HgII), oxidised Hg species associated with soluble aerosols (HgIIaq), and Hg associated with insoluble aerosol particles, HgP. The model horizontal resolution is a spectral T42 grid (approximately 2.8° by 2.8°), with an hybrid-sigma pressure system with 19 non equidistant vertical levels up to 10 hPa. The model includes offline anthropogenic emissions from the POET emission inventory. This is an extension of EDGAR 3 emission dataset (Granier et al. 2005; Peters et al. 2003) that includes biogenic emissions from the GEIA inventories (http://www.geiacenter.org). Mercury emissions from oceans, forest fires and from biogenic activities are mapped to the respective CO emissions from the POET inventory. The anthropogenic mercury emissions used are from the AMAP emission inventory (Pacyna et al. 2006). See Jung et al., 2009 (and De Simone 2013, this issue) for the full description of the model.

Moreover, an alternative set of boundary concentrations for mercury was taken from the Global EMEP Multi-media Modeling System (GLEMOS) (Travnikov and Ilyin, 2009). GLEMOS is a multi-scale simulation platform developed for assessment of environmental dispersion and cycling of different classes of pollutants including mercury. The base model grid on a global scale has horizontal resolution 1°×1°. In the vertical the model domain covers the height up to 10 hPa and consists of 20 irregular terrain-following sigma layers. Atmospheric chemical scheme of the model includes redox reactions of mercury transformations both in gaseous phase and in aqueous phase of the cloud environment. Major atmospheric oxidants considered by the model include ozone, hydroxyl radical as well as reactive halogens (Br and BrO) over the polar regions. The mercury concentrations from GLEMOS were used as default boundary conditions because GOM and PBM concentrations were lower than in the ECHMERIT run and led to better agreement with observations.

2.5 Observations

For the evaluation of the CTM results observations from European measurement stations from the EMEP network are used (CCC, 2013). In total, 24 rural stations measure wet deposition on a monthly basis and 14 measure atmospheric concentrations of mercury. However, only 18 deposition stations and 10 concentration stations with more than 75% data availability were taken into account here (Table 1). Observations of atmospheric mercury were only available for GEM at all stations except DE02. These measurements are based on the Tekran 2537 Instrument, which is the global standard for gaseous mercury detection. GEM measurements are performed on an hourly basis but usually reported as daily averages. Only at Waldhof (DE02), a station operated by the German Umwelt Bundesamt (UBA), quasi-simultaneous measurements of GEM, GOM, and PBM are performed. At Waldhof, a Tekran Instrument with a speciation unit collects GOM on a

potassiumchloride (KCl) treated denuder and PBM on a particle filter, over the duration of 150 minutes. During the collection time GEM is measured and every 150 minutes the GEM measurement is stopped and GOM and PBM are measured (Weigelt et al., 2013). This leads to an average of 7 GOM and PBM observations per day.

At all EMEP stations wet deposition is measured with wet only samplers. This has the advantage, that the observed mercury deposition is not influenced by dry deposition. However, no wet and dry deposition samplers are operated that could yield information on the dry deposition. At most EMEP stations the wet deposition is aggregated and measured once per month. Only at Waldhof, weekly wet deposition measurements are available. The measurements are performed according to the EMEP standard operation procedures (Aas, 2006), which are based on the ambient air quality standard method for the determination of mercury deposition (NEN-EN 15853, 2010).

Station	Namer	C	D	Latitude deg N	Longitude deg E	Altitude m asl
BE14	Koksijde		X	51.45	3.3	4
DE01	Westerland		X	54.12	8.30	12
DE02	Waldhof	X	X	52.80	10.75	74
DE03	Schauinsland		X	47.90	7.90	1205
DE08	Schmücke	X	X	50.65	10.77	937
DE09	Zingst	X	X	54.43	12.73	1
ES08	Niembro		X	43.43	-4.85	134
IE31	Mace Head	X		53.32	-10.28	5
FI36	Pallas (Matorova)	X	X	68.00	24.23	340
GB13	Yarner Wood		X	50.59	-3.70	119
GB17	Heigham Holmes		X	52.72	-1.62	0
GB48	Auchencorth Moss	X	X	55.78	3.23	260
GB91	Banchory		X	57.07	-2.53	120
NL91	De Zilk		X	52.30	4.50	4
NO01	Birkenes	X	X	58.38	8.25	190
PL05	Foia	X		37.32	8.90	902
SE05	Bredkälen		X	63.85	15.33	404
SE11	Vavihill	X	X	56.02	13.15	175
SE14	Råö	X	X	57.39	11.90	5
SI08	Iskrba		X	45.57	14.87	520

Table 1: EMEP stations used for model evaluation. Location is given in decimal degrees, altitude in m. The columns C and D indicate whether Concentration and Deposition measurements are available.

3. Results and Discussion

3.1 Evaluation of atmospheric mercury concentrations

About 99% of the total atmospheric mercury is in the form of GEM (Gay et al., 2013). The background concentration of GEM in the northern hemisphere varies between 1.5 and 1.8 ng/m³ (UNEP, 2008). It has been shown in previous studies that global models are able to reproduce the global background concentrations of GEM within a range of ±15% (Ryaboshapko et

al., 2007b, 2007c; Bullock et al., 2008). For GOM and PBM however, models have been found to generally overestimate observations (Zhang et al., 2012b). Recent studies indicate, that the main driver for the overestimation of GOM is the current emission split assumed in the AMAP inventory (Zhang et al. 2012c, Kos et al., 2013). Because GEM is transported on a hemispheric scale the concentrations in a regional model domain are dominated by the boundary conditions. Hence, in this study no in-depth analysis of observed and modelled GEM concentrations was carried out. A comparison of CMAQ-Hg results with GEM measurements from EMEP stations for 2009 was in the range of previous studies. Generally, CMAQ-Hg underestimated the hourly GEM concentrations by 8.3% in the CCLM and 7.5% in the WRF run (Table 2). An investigation of hourly GEM measurements showed that the bias can mainly be explained by the fact that the model is not able to reproduce some pronounced GEM concentration peaks. Furthermore, in Spring the global models have low GEM concentrations due to mercury depletion events over the Arctic Ocean. This leads to too low GEM concentrations in CMAQ-Hg during spring, because the re-emission of deposited mercury from the ocean is currently not implemented into CMAQ-Hg. To determine the flux of mercury out of the atmosphere into marine and terrestrial ecosystems the concentrations of the oxidized mercury species GOM and PBM, which have a much shorter lifetime than GEM, is of major concern. However, there are only few measurements of speciated mercury available. For the year 2009 only one station in Europe (Waldhof) observed GEM, GOM, and PBM continuously.

At Waldhof, CMAQ-Hg overestimated PBM by 84% in the CCLM run and 120% in the WRF run. For GOM the model strongly overestimated the annual mean concentrations by a factor of 7 (CCLM) and a factor of 10.5 (WRF) (Fig. 1). In the model 60% of the total oxidized mercury (TOM) is PBM and 40% GOM. In the observations PBM makes up 86% of TOM. This indicates, that the split between GOM and PBM in the emission data set needs to be adjusted as in the current model setup the primary emissions are the single largest source of GOM and no other source (i.e. gas-particle partitioning and oxidation of GEM) is large enough to explain this finding. As discussed in Section 2.2, this is assumption is backed up by recent aircraft based measurements at a German coal fired power plant (Weigelt, p.c.). Also, in a recent study Kos et al. (2013) observed large improvements in model performance, both for concentration and wet deposition, by reducing the amount of GOM emissions from power plants from 40% to 2%. Moreover, the split of 50% between GOM and PBM in the chemical mechanism for GEM oxidation might need to be revised (Amos et al., 2011). This is in line with the findings of Calvert and Lindberg (2005), who suggested that the oxidation is overestimated by the current reaction rates. Depending on the model setup CMAQ-Hg overestimated TOM by a factor of 2 to 3 (Table 2). However, the model is able to reproduce the variability of PBM. The higher bias for the variability of GOM can be explained by the fact that the measurements are very close to the detection limit of 0.4 pg/m³. In the analysis all observed GOM concentrations below 0.4 pg/m³ were set to the detection limit and thus GOM concentrations do not exhibit a normal distribution.

	Observation			Model (CCLM)			Model (WRF)			low GOM CCLM		low GOM WRF	
	GEM	GOM	PBM	GEM	GOM	PBM	GEM	GOM	PBM	GOM	PBM	GOM	PBM
Mean	1.7	1.6	9.6	1.6	11.0	19.4	1.6	16.8	23.8	2.1	15.4	2.9	18.4
Median	1.6	0.6	6.2	1.5	9.6	13.7	1.6	13.3	18.1	1.6	11.3	2.2	9.6
Std. (hourly)	0.3	2.4	12.2	0.3	7.7	15.5	0.2	13.1	17.3	1.7	15.4	2.4	12.2
MNB (hourly)	-	-	-		9.7	8.9		15.2	12.2	0.5	5.7	1.4	8.8
MNE (hourly)	-	-	-		10.1	13.8		15.4	17.2	1.9	11.9	2.4	14.7
R^2 (bi-weekly)	-	-	-		0.03	0.64		0.02	0.04	0.07	0.61	0.21	0.09
R^2 (diurnal)	-	-	-		0.01	0.43		0.01	0.34	0.64	0.46	0.70	0.18

Table 2: Statistical analysis of modelled and observed speciated mercury concentrations at Waldhof (DE02) for 2009. All values are based on hourly measurements of GEM and 3-hourly measurements of GOM and PBM. Units are ng/m³ for GEM and pg/m³ for GOM and PBM. The last two columns relate to an alternative CMAQ-Hg run with no GOM emissions and no chemical production of PBM. Statistical values shown are the mean normalized bias (MNB) and mean normalized error (MNE) based on hourly values as well as the correlation for the annual cycle (based on bi-weekly averages) and the diurnal cycle (based on 3-hourly values). The measurement of GOM and PBM is divided in 3 hours of sampling and 1 hour 25 minutes of analysis. Thus, there are roughly 5 measurements per day and about 77 measurements for each hour per year of observation.

Statistics for a second set of alternative model runs without any GOM emissions and without any PBM production from

oxidation are given in Table 2 *'low GOM CCLM/WRF run'*. This model setup led to a better agreement with observed GOM and PBM concentrations at Waldhof. Furthermore, the model can now reproduce the diurnal cycle of GOM. GOM exhibits a strong diurnal cycle, which can be explained by the increased oxidation of GEM during day time (Weigelt et al., 2013). The diurnal GOM cycle in the default CMAQ-Hg model run, however, was mainly influenced by primary emissions. PBM concentrations have no pronounced diurnal cycle both in the model and the observations. This leads to the fact, that the diurnal correlation for PBM is strongly influenced by small hourly fluctuations. On a seasonal scale, PBM concentrations have an annual cycle which could be traced back to increased primary emissions from the combustion of fossil fuels in winter in combination with lower PBL heights. For GOM, the model as well as the observations show higher concentrations during summer. This can be explained by increased oxidation. However, also during winter high GOM concentration episodes have been observed. These episodes are the main reason for the low intra-annual correlation between model and observation. In the standard CMAQ-Hg runs GOM and PBM concentrations are mostly dominated by the primary emissions. In these runs the production of PBM by the oxidation mechanism leads to an overestimation of PBM concentrations during summer. For GOM the boundary conditions had a strong influence on modelled concentrations only during summer. This indicates, that in this period oxidation of GEM over the Atlantic is overestimated in the global models. The GLEMOS model was chosen as source for boundary conditions, because it predicts lower GOM and PBM concentrations compared to other global models. Still, the oxidized mercury concentrations given by GLEMOS are considered too high and alternative global mercury concentration datasets led to even higher GOM and PBM concentrations over Europe.

3.2 Evaluation of modelled precipitation and it's impact on deposition

Much more than for atmospheric concentrations, it is of high interest for dry and wet deposition whether the oxidized mercury fraction is dominated by GOM or PBM. GOM can also undergo significant dry deposition while PBM is almost exclusively wet deposited. This is due to the fact that PBM is mainly associated with particles with a diameter between 0.1 and 2.5µm. These particles represent the highest volume concentration of atmospheric particulate matter. The overestimation of atmospheric PBM concentrations leads to the assumption that also the Hg concentration in rain water should be overestimated by the model. Whether the deposition flux is also overestimated is highly dependent on the quality of the precipitation fields created by the meteorological models. For this reason, CMAQ-Hg was run with two alternative sets of meteorological fields from two meteorological models. In a first approach, the calculated monthly precipitation values for 2009 were compared to reanalysis data (Haylock et al., 2008). This evaluation showed that CCLM generally gives very good results for central Europe. During most of the year the absolute bias of monthly precipitation in this region is below 20 mm. However, during the summer months CCLM calculates too low amounts of precipitation. This effect is especially pronounced in Eastern Europe. Moreover, CCLM strongly underestimates the precipitation on the Iberian peninsula during autumn with monthly biases up to -50 mm. Finally, in Norway and Sweden CCLM exhibits a few spots with extremely large precipitation overestimations in spring. The precipitation fields generated with WRF have much higher annual precipitation over the whole domain. Similar to the CCLM run WRF predicts too low precipitation over Eastern Europe and Russia during summer time and performs best over central Europe. Generally, WRF overestimates precipitation over the Iberian peninsula and Scandinavia with around 50mm per month. The monthly precipitation bias for the two models are given in the supplementary material.

The main focus of this study is the deposition of mercury. Thus, only stations where the total precipitation is correctly represented in the meteorological fields are used for further analysis. Otherwise, it would be difficult to distinguish between an evaluation of the meteorological fields and an evaluation of the CTM. Figure 2 shows that for most stations the models underestimate monthly precipitation. Generally, WRF predicts higher amounts of precipitation than CCLM and is in better agreement with monthly observations. Moreover, the models are generally biased to underestimate precipitation. The highest underestimation of precipitation is found for the mountain stations Schauinsland (DE03, altitude 1200m) and Schmücke (DE08, altitude 937m). Here, it can be assumed that the model is unable to reproduce convective or orographic precipitation because of the coarse model resolution. Moreover, the deviation from observations is largest for coastal areas with complex topography where both land, and open ocean fall into a single model grid cell (GB13, NO01, SE14). However, the models perform surprisingly well at all other coastal measurement stations (DE01, SE11, GB91, NL91). The only station with an overestimation of annual total precipitation by both models are FI36 and SE14. Yet, the precipitation collected by the wet deposition container does not necessarily represent the actual precipitation at a station due to the sampling duration and days without sampling. For example, this is the reason why the precipitation at the station FI36 is strongly overestimated by the model. Hence, a direct comparison of observed and modelled precipitation based on the

monthly measurements of precipitation collected by the deposition sampler is subject to additional methodological uncertainties. A comparison to independent continuous precipitation observations is much better suited to evaluate the meteorological model, but not to evaluate the deposition calculated by the CTM. This is due to the fact, that the observed wet deposition is measured as a concentration in rain and needs to be transformed into a deposition flux based on the total precipitation per measurement. Additionally, because wet deposition is a non-linear process the actual amount of precipitation collected by the deposition sampler must be used for this purpose.

Finally, the long sampling periods impair the comparison of observed and modelled precipitation. The EMEP stations report only monthly precipitation and deposition values. Because most of the deposition occurs in the beginning of the precipitation event, two short events will lead to higher deposition fluxes than one long single event with the same amount of precipitation. The averaging over long time spans can conceal the structure of the precipitation events and thus possibly falsifies the evaluation of modelled precipitation. For example, one model can be better at predicting the monthly total precipitation but worse at predicting high resolution precipitation patterns. At the EMEP station DE02 (Waldhof) weekly precipitation and deposition values from the deposition sampler as well as daily precipitation values from an independent sampling system could be obtained. This allows for a more detailed evaluation of the model at this particular point in the domain. Figure 3 depicts the observed and modeled precipitation as monthly, weekly, and daily averages. It can be seen, that the agreement of monthly values does not necessarily represent similar daily precipitation patterns. Generally, WRF is better at reproducing large precipitation events, but often overestimates precipitation in dry periods. For the CCLM precipitation fields it is exactly the other way around. To illustrate this, figure 4 gives the frequency distribution of daily precipitation amounts for both models as compared to the observations. CCLM is able to reproduce dry periods without precipitation but often fails to get larger precipitation events. For example, WRF predicts strong precipitation events in August, while CCLM is able to reproduce the dry conditions during August (Fig. 3). In May for example the monthly precipitation is dominated by a strong precipitation event with 40mm on one day and three medium events with 10mm of rain. CCLM is able to roughly reproduce this pattern and thus is in good agreement with the monthly total precipitation. A similar picture is found for January where the monthly precipitation at Waldhof is dominated by a single rain event. This is reproduced by WRF but not by CCLM. In contrast, WRF is then unable to reproduce the dry situation during the rest of the month and thus overestimates the precipitation in January. As discussed above, wet deposition is a non-linear process because the precipitation quickly scavenges the pollutants from the atmosphere. Thus, it is more important for the meteorological models to properly reproduce dry days and small precipitation events (Fig. 4). While the underestimation of a large precipitation event has a much smaller influence on monthly deposition than on monthly precipitation.

Because of this, one result of the analysis of modelled monthly precipitation and deposition averages is that similar amounts of precipitation can lead to different deposition fluxes (e.g. ES08, GB48) and different amounts of precipitation can lead to similar deposition fluxes (e.g. GB13, NL91) (Fig. 2). Again, this shows that only little information can be acquired from monthly average values. Looking at the high resolution data for the Waldhof (DE02) station it is possible to analyse the relationship between precipitation and deposition. Figure 5 gives an excerpt of figure 3 for the months March through May. These months represent a wide variety of precipitation events. Moreover, they are used to illustrate the influence of the different meteorological fields on modelled mercury deposition.

In March, both models exhibit a very good agreement with the observations for monthly and weekly precipitation averages with a NMB between +7% (CCLM) and +8% (WRF) (Fig. 5). But, this picture is not consistent with the daily precipitation patterns. In March CCLM is able to reproduce a high precipitation event on the 22nd of March as well as a dry period between the 13th and the 20th of March. WRF, on the other hand, underestimates the high precipitation event but predicts precipitation during the dry period as well. These two errors, too much rain during the low precipitation period and too little rain during a pronounced precipitation event, cancel out when looking at monthly or even weekly precipitation averages. Because of the non-linear nature of scavenging the overestimation of precipitation during this period leads to much higher total monthly average depositions in the CMAQ-Hg WRF setup (+70%) compared to the CCLM run.

During the first three weeks of April no rainfall at all occurred at Waldhof. The observed deposition for this month occurred on the last three days. On average, both meteorological models predict even lower total precipitation for April. But instead of a single strong event at the end of the month the models give tiny bits of precipitation throughout the month. Still, the modelled deposition for April is in good agreement with observations, which is the lowest monthly value at Waldhof in 2009.

At last, a detailed analysis for May is carried out. This month is of interest because the WRF model manages to predict the total precipitation but overestimates the deposition by a factor of 4.5. Meanwhile, the CCLM CMAQ-Hg run is able to reproduce the deposition but CCLM missed 70% of the precipitation in May. The daily precipitation measurements show

that the rain column in May is dominated by a single precipitation event on the 20th which contributed 50% of the monthly precipitation. CCLM has no precipitation at the 20th of May but manages to reproduce the precipitation pattern for the rest of the month. Together with the general overestimation of deposition due to too high GOM concentrations the CCLM run has a relatively low deposition bias of +29%. WRF can partially reproduce the high precipitation event on the 22nd. However, the meteorological model has too high precipitation during the second week of May which was very dry. In total, WRF is able to reproduce the total precipitation for May but leads to an large overestimation of wet deposition of +124%. These findings illustrate the difficulty of an evaluation of modelled wet deposition because of competing effects of model errors in precipitation and atmospheric concentrations. Especially for the precipitation, observations with a high temporal resolution are needed in order to evaluate the quality of the meteorological fields used for the CTM run. Ideally, the duration and amount of precipitation for each rain event is recorded separately.

3.3 Evaluation of mercury deposition

Figure 6 depicts the normalized mean bias for precipitation, deposition flux, and mercury concentration in rain for 2009 at 18 EMEP stations for the default and low GOM CMAQ-Hg runs (using ensemble values for CMAQ-Hg runs with CCLM and WRF meteorology). Most of the modelled annual wet depositions (78% default runs, 89% low GOM runs) are within a factor of 2 of the observed values. For monthly average values this number is between 83% (low GOM ensemble), 75% (CCLM default), 75% (WRF low GOM), 58% (CCLM low GOM), 58% (default ensemble), and 33% (WRF default). The model performance is similar for most months, but poor for March and November. Furthermore, some deductions can be drawn from the structure of the bias. For the WRF runs, the low GOM CMAQ-Hg setup leads to a decreased bias, while for the CCLM runs the bias increases. A more thorough analysis of this reveals that the default CCLM run produced correct wet depositions due to the interaction of different effects. On the on hand, CCLM has too low precipitation values and on the other hand the default runs lead to too high GOM concentrations. These two biases cancel each other out. Looking at the ensemble model results for the two default and the two low GOM runs one can see a significant decrease of bias and error for modelled monthly wet deposition values in the low GOM setup. The Mean Normalized Bias (MNB) drops from 0.79 to 0.03 and the Mean Normalized Error (MNE) decreases from 0.80 to 0.37. More importantly, in the low GOM run the bias of modelled wet deposition and concentration in rain are now in better agreement with the precipitation bias with exception of two Swedish stations SE05 and SE14 (Fig. 6). This indicates, that the modifications applied for the low GOM CMAQ-Hg runs improved the overall model performance.

To further analyse the differences between the default and the low GOM CMAQ-Hg runs, the seasonal absolute values (Fig. 7) and the relative changes (Fig. 8) for different mercury species wet and dry deposition are investigated. First of all, it can be seen that for all species, the relative differences are higher in winter time than during summer (Fig. 8). This is due to the lower influence of GEM dry deposition during winter (Fig. 7). More importantly, the relative total deposition differences are non-linear throughout the year. The main factor for the different deposition patterns in the two CTM scenarios is the strongly reduced dry and wet deposition of GOM. Speaking in absolute units, in most regions the main factor is the reduced dry deposition of GOM in the low GOM CMAQ-Hg runs. The deposition of PBM, which is mainly due to wet deposition, exhibits a much smoother, more linear difference between the two model setups. These findings can be explained by the shift of the atmospheric GOM to PBM ratio in the model which leads to less deposition near major source areas and more long range transport. Therefore, the improvement of model results seems directly linked to the decreased atmospheric concentration of GOM.

However, so far we only validated the improvement of modelled GOM concentrations for the surface layer. Because the wet deposition is dependent on the integrated air column concentration below the cloud top, it is also of interest to investigate the vertical structure of GOM and PBM. First of all, the area of interest needs to be determined. An analysis of model cloud top height revealed that 90% of the precipitation takes place below 2000m and more than 80% is inside the PBL. Therefore, the wet deposition of mercury is dominated by the GOM and PBM concentration inside the PBL. Unfortunately, the current measurement techniques do not allow for high resolution vertical measurements of these species. The atmosphere inside the PBL is characterized by turbulent mixing and usually exhibits low concentration gradients. Vertical profiles of GEM, for example, show constant values inside and lower concentrations above the PBL (Swartzendruber et al., 2008). Aircraft based measurements of GOM in the US have shown slightly higher concentrations above the PBL and large GOM peaks in high altitudes between 3000m and 9000m (Sillman et al., 2007). The slightly higher concentrations above the PBL can be explained by the increased radiation above the cloud layer which leads to a more oxidative environment. This GOM peak is also visible in the model results both of the default and low GOM runs. Moreover, it is mostly located above the cloud top.

Because of the low particle volume concentration in the free troposphere, other than for GOM a decrease of PBM is assumed above the PBL (Kvietkus, 1995). This confirms the assumption that the too high GOM concentration modelled inside the PBL due to the large GOM fraction in current emission inventories, are the main factor for the overestimation of mercury concentrations in rain. Thus, an underestimation in precipitation generally leads to better agreement with observed wet deposition fluxes, which in term benefits the CMAQ-Hg run using the CCLM meteorological fields.

Because of the better agreement with observations, we chose to plot absolute deposition results from the low GOM runs (Fig. 7). It can be seen, that in summer dry deposition of GEM is the largest fraction of the total deposition. While during winter the dry and wet deposition of GOM and PBM are more important. Although, PBM concentrations in the atmosphere are higher than GOM concentrations by a factor of 7, the absolute wet deposition of both species is similar. Due to the small deposition velocity of the particles PBM is associated with, the dry deposition of PBM plays only a minor role. Thus, GOM is the more important specie for total deposition of oxidised mercury. However, in regions with high precipitation amounts and large mercury sources the wet deposition of PBM can become the largest fraction. One region of particular interest is south of the Alps, especially the Po valley, where wet deposition in the model is much higher than dry deposition and the deposition of PBM is about twice as high as that of GEM.

Finally, the wet deposition at the different EMEP stations was compared to the modelled dry deposition (Table 3). At Waldhof, mercury deposition is split almost evenly into wet TOM deposition (30%), dry TOM deposition (32%) and dry deposition of GEM (38%). For the 18 EMEP stations, at which mercury wet deposition was observed during 2009, the modelled ratio of dry to wet deposition lies in the range of 0.6 to 5.0. These values are in the range of ratios observed in the U.S., which are in the range of 0.8 to 4.8 (Zhang et al., 2012). On average the model results indicate that over Europe 33% of the total mercury deposition is due to wet deposition, 35% due to dry deposition of oxidized mercury, and 32% due to dry deposition of GEM. The average dry to wet deposition ratio is 2.0.

Station	GOM+PBM	net GEM	total dry	wet	dry/wet	Precip [mm]
BE14	3.3	3.8	7.1	2.7 (28%)	2.6	650
DE01	2.9	3.5	6.4	3.9 (38%)	1.6	740
DE02	3.3	4.1	7.4	2.9 (28%)	2.6	638
DE03	3.0	4.3	7.4	5.1 (41%)	1.5	1382
DE08	4.0	4.1	8.1	3.1 (28%)	2.6	1310
DE09	2.3	0.8	3.1	3.4 (53%)	0.9	561
ES08	3.5	1.2	4.7	1.8 (27%)	2.6	1028
FI36	3.2	3.0	6.2	1.2 (17%)	5.2	238
GB13	4.1	3.8	7.9	3.3 (29%)	2.4	1296
GB17	2.4	1.5	3.9	2.2 (36%)	1.8	462
GB48	2.1	2.1	4.2	3.4 (45%)	1.2	679
GB91	2.1	2.1	4.2	3.8 (47%)	1.1	777
NL09	3.4	3.0	6.4	2.8 (30%)	2.3	719
NO01	2.7	4.1	6.8	3.8 (36%)	1.8	1790
SE05	2.7	3.4	6.1	1.3 (18%)	4.7	412
SE11	3.2	3.7	6.9	3.6 (34%)	1.9	605
SE14	3.2	2.3	5.5	4.4 (44%)	1.3	458
SI08	5.4	0.8	6.2	10.2 (62%)	0.6	1254

Table 3: Modelled annual dry deposition of (GOM+PBM) and (GEM) [µg/m²], total mercury wet deposition [µg/m²] and observed annual precipitation [mm] for 18 EMEP stations. The percentage in brackets indicates the fraction of wet deposition compared to total mercury deposition. The EMEP stations are described in Table 1.

3.4 Wet deposition sensitivity on input parameters

To determine the influence of input parameters on the modelled deposition of mercury a sensitivity analysis has been performed. At first, the influence of the sampling rate of precipitation measurements was investigated. For monthly samples a weak correlation between precipitation and deposition was found with R^2=0.28 (CCLM), R^2=0.30 (WRF) for modelled and R^2=0.36 for observed values. The usage of weekly data already gives much better correlation coefficients with R^2=0.52 (CCLM), R^2=0.49 (WRF) for modelled and R^2=0.59 for observed values. Deposition measurements are not available on a daily basis, thus no correlation can be calculated for higher sampling rates. Anyhow, due to the discrete structure of high resolution precipitation measurements it was not possible to find a correlation for these data.

As discussed in the previous section, similar averaged precipitation fields can lead to different deposition fluxes and vice versa. Thus, monthly average values seem to be an unreliable measure to evaluate modelled deposition fields. To better understand the influence of the different driving factors, Figure 9 illustrates the relationship of precipitation, atmospheric concentration, and deposition. On the three dimensional scatter plots the bias between model and observation for these three values is given based on weekly measurements. The bias of the deposition is depicted in the third dimension using a color palette. The shaded area gives the range in which, assuming a linear relationship between the three input parameters, the combined bias of precipitation and concentration is below a factor of 2. The green dots, which illustrate a high agreement of modelled and observed wet deposition are mostly aligned along this shaded area. This supports the assumption of a quasi-linear relationship between precipitation, atmospheric concentration, and deposition. Moreover, this might be an explanation for the non-linear relationship between precipitation bias and deposition bias found in earlier studies (Bullock et al., 2009) and illustrates the importance of speciated mercury measurements for model evaluation. Figure 9a and 9b show results for CMAQ-Hg runs using the different meteorological models. Figures 9c and 9d depict results from low GOM CMAQ-Hg runs in which the atmospheric concentrations of GOM and PBM were severely reduced by removing all primary emissions of GOM and without any PBM from the oxidation from GEM. Especially for the WRF run, which has higher precipitation levels, the reduction of atmospheric GOM and PBM leads to a better agreement of modelled and observed deposition fluxes (Figs. 9a, 9d). In the CCLM based CMAQ-Hg runs, the modelled annual mercury deposition at Waldhof (observation 4.6 µg/m²) drops from 4.4 µg/m² to 2.9 µg/m². It drops from 10.9 µg/m² to 6.4 µg/m² for the runs using WRF meteorological fields.

A correction based on the bias of weekly precipitation had a strong effect on the correlation between modelled and observed depositions (Table 4). This adjustment method, however, increased both bias and error. This results are in accordance with the findings of Bullock et al. (2009). Using the atmospheric concentrations of GOM and PBM to adjust the modelled weekly deposition had almost no effect on the correlation and only in the WRF run the bias improved considerably from -123 ng/L to -23 ng/L. When combining the two parameters (precipitation and atmospheric concentrations) the best results for adjusted modelled depositions were obtained for all statistical values (Table 4). This further indicates the importance of speciated mercury measurements for the evaluation of deposition fields.

	CCLM - default				CCLM - low GOM				WRF - default				WRF - low GOM			
	default	conc	precip	combo	default	conc	precip	combo	default	conc	precip	combo	default	conc	precip	combo
R^2	0.22	0.22	**0.82**	**0.83**	0.14	0.39	**0.89**	**0.91**	0.18	0.16	**0.65**	**0.63**	0.17	0.23	**0.75**	**0.71**
bias [ng/m²]	**1**	-55	66	-32	-32	-52	**2**	-30	123	**-23**	143	**-19**	35	**-21**	38	**-19**
error [ng/m²]	57	62	83	**36**	60	65	38	**36**	151	64	155	**43**	85	60	63	**40**

Table 4: R^2 scores, mean bias, and mean error of modelled and observed deposition fields at Waldhof (DE02). All data is based on weekly values for 2009. The observed mean deposition for 2009 is 4.7 µg/m². A correction of the modelled weekly wet depositions by means of the precipitation bias (observation/model) leads to a significant increase in correlation but also to increased bias and error. A correction using the bias of observed and modelled atmospheric TOM concentrations decreased the deposition bias and error. Generally, the combined correction with both vaues (combo) leads to the best agreement with observations for all model setups.

4. Conclusion

In the course of this paper it has been shown that a regional application of the Chemistry Transport Model (CTM) CMAQ-Hg is capable to reproduce atmospheric concentrations and wet deposition fluxes of mercury for Europe. Concerning atmospheric concentrations, the model was able to reproduce the background concentration of GEM and PBM. The GEM concentrations were slightly underestimated (-8%) by the model results are inside the range of previous model exercises. Concerning PBM, the model could reproduce the annual concentrations within a factor of 2.

For the oxidized mercury species GOM and PBM only a single station in Europe has performed continuous measurements for the year 2009. At the Waldhof station (DE02), which is an EMEP station operated by the German Umwelt Bundesamt (UBA) atmospheric mercury concentrations are measured on a three-hourly basis and wet deposition is measured with a weekly sampling interval. A comparison of speciated mercury concentrations measured at Waldhof to similar stations in the US show background values for GEM, PBM, and GOM in the same order of magnitude. Although, the GOM concentrations at Waldhof are even lower than at other stations. The modelled PBM concentrations were too high but still mostly within a factor of 2 to observations. The model was able to reproduce a weak annual cycle of PBM concentrations with higher values during winter time. This increase could be attributed to higher fossil fuel burning during the cold season. Both model and observations indicate no diurnal cycle of PBM concentrations. GOM was strongly overestimated by a factor of 10 compared to observations. Generally, modelled GOM concentrations were in the same range as PBM concentrations. Measurements indicate very low GOM concentrations at Waldhof throughout the year with a mean of 1.3 pg/m³ and a median concentration of 0.6 pg/m³. This is just slightly above the detection limit of 0.4 pg/m³ of the three-hourly measurements. However, the GOM concentrations at Waldhof in 2009 were exceptionally low and average values in 2010 and 2011 went up to 3 pg/m³.

Based on observations from aircraft measurements in the vicinity of a major coal fired power plant is was assumed that the current speciation profiles for oxidized mercury need to be adjusted. Furthermore, it was assumed that the oxidation of GEM does not directly produce PBM and thus PBM has been removed as a product in the models chemistry mechanism. Low GOM CMAQ-Hg runs with the described setup lead to better agreement of modelled and observed atmospheric GOM concentrations independent of the used meteorological fields. Besides, the model was now able to reproduce the diurnal cycle of GOM, which is subject to an increased chemical production during day time. Additionally, the variability of modelled hourly GOM (2.1) and PBM (13.8) concentrations showed an excellent agreement with the observed variability of these species (2.4 and 12.2). Finally, without the chemical production of PBM during summer, PBM was not overestimated by the model during this season anymore.

To evaluate the wet deposition modelled by CMAQ-Hg, the CTM was run with two alternative meteorological fields as input datasets. Firstly, the COSMO-CLM (CCLM) model was used. CCLM was generally underestimating precipitation in Europe. For several stations the bias was up to -50%. The missing precipitation in CCLM was attributed to strong precipitation events. Apart from this, CCLM was very adept at reproducing dry episodes and small precipitation events. This proved to be of high importance for the calculation of wet deposition fluxes. Secondly, the Weather Research and Forecast (WRF) model was utilized. The WRF data set was much better in reproducing the annual total precipitation for 2009. However, the model often overestimated precipitation during dry episodes finally leading to too high wet deposition fluxes.

The comparison of modelled and observed precipitation averaged over different sampling intervals (monthly, weekly, daily) revealed that for the evaluation of wet deposition a high resolution dataset with at least daily precipitation measurements is of utmost importance. Looking at aggregated precipitation values, similar model results could lead to different deposition values and vice versa. Only a detailed analysis of daily precipitation totals and weekly deposition samples could give an insight into the mechanisms and interactions of the different input datasets and model parameters. At Waldhof the CMAQ-Hg CCLM run, which underestimated the annual precipitation by 25% was able to reproduce (4.4 µg/m²) the observed wet deposition flux of 4.6 µg/m². The CMAQ-Hg WRF run, which slightly overestimated the annual total precipitation by 9% overestimated the deposition flux by more than a factor of 2 (10.9 µg/m²). This proves the strong influence of the meteorological fields on modelled deposition values. Furthermore, a low annual bias was not necessarily linked to a low weekly error, indicating that the extinction of different errors can lead to a good modelled annual average value. This shows, that because of the non-linear nature of sub-cloud scavenging it is not possible to evaluate modelled mercury wet deposition with precipitation measurements only. Generally, the low GOM CMAQ-Hg setup lead to a decrease of the weekly error of modelled wet deposition. More importantly, a combined analysis of the biases of precipitation and atmospheric concentrations was able to explain the bias of modelled wet deposition of mercury. The adjustment of modelled weekly

depositions based on model biases of weekly precipitation and atmospheric concentrations could significantly increase correlation, bias, and error of the deposition fields. This was not possible with an adjustment based on only one of the two parameters. Hereby, the precipitation had the largest influence on the correlation and the atmospheric concentrations had the largest influence on bias and error. Finally, the modelled dry to wet deposition ratio with this model setup was in a similar range as ratios observed in the U.S.. No model comaprison of dry depositions could be performed due to a lack of measurements.

Acknowledgements

We want to thank Elke Bieber from the German Umwelt Bundesamt (UBA) and Andreas Schwerin from the Waldhof station for their support and the various measurement data used in this publication. Further, our thanks go to Andreas Weigelt, who operates the Tekran instruments at Waldhof. Moreover, we thank EMEP for the various European measurement data. Finally, we acknowledge the climate dataset from the EU-FP6 project ENSEMBLES (http://www.ensembles-eu.org) and the data providers in the ECA&D project (http://eca.knmi.nl). Finally, we want to thank Franz Slemr for fruitful discussions on the topic.

References

Aas, W., (ed.) (2006). Data quality 2004, quality assurance, and field comparisons. EMEP/CCC Report 4/2006, Norwegian Institute for Air Research (NILU), Norway.

Amos, H.M., Jacob, D.J., Holmes, C.D., Fisher, J.A., Wang, Q., Yantosca, R.M., Corbitt, E.S., Galarneau, E., Rutter, A.P., Gustin, M.S., Steffen, A., Schauer, J.J., Graydon, J.A., St. Louis, V.L., Talbot, R.W., Edgerton, E.S., Y. Zhang, Sunderland, E.M., (2012). Gas-particle partitioning of atmospheric Hg(II) and its effect on global mercury deposition Atmos. Chem. Phys., 12, 591-603, doi:10.5194/acp-12-591-2012.

Amos, H.M., D.J. Jacob, D.G. Streets, and E.M. Sunderland, (2013). Legacy of all-time anthropogenic emissions on the global mercury cycle. Global Biogeochemical Cycles, 27, 2, 410-421, doi:10.1002/gbc.20040.

Baker, K.R., Bash, J.O., (2012), Regional scale photochemical model evaluation of total mercury wet deposition and speciated ambient mercury. Atmos. Environ. 49, 151-162.

Bash, J.O., 2010. Description and initial simulation of a dynamic bidirectional air-surface exchange model for mercury in Community Multiscale Air Quality (CMAQ) model. JO Bash Journal of Geophysical Research 115 (D6), D06305

Bieser, J., Aulinger, A., Matthias, V., Quante, M., Builtjes, P., (2011a). SMOKE for Europe – adaptation, modification and evaluation of a comprehensive emission model for Europe. Geosci. Model Dev. 4, 1–22, doi:10.5194/gmd-4-1-2011.

Bieser, J., Aulinger, A., Matthias, V., Quante, M., Denier van der Gon, H.A.C., (2011b). Vertical emission profiles for Europe based on plume rise calculations. Environ. Pollut. 159, 2935-2946. doi:10.1016/j.envpol.2011.04.030.

Bullock Jr O.R., Brehme K.A., (2002). Atmospheric mercury simulation using the CMAQ model: formulation description an analysis of wet deposition results. Atmos Environ 36:2135–46.

Bullock, O.R., Atkinson, D., Braverman, T., Civolo, K., Dastoot, A., Davignon, D., Ku, J.Y., Lohmann, K., Myers, T.C., Park, R.J., Seigneur, C., Selin, N.E., Sistla, G., Vijayaraghavan, K., (2008). The North American Mercury Model Intercomparison Study (NAMMIS): Study description and meodel-to-model comparisons. Journal of Geophysical Research Atmospheres, 133 D17.

Bullock, O.R., Atkinson, D., Braverman, T., Civolo, K., Dastoot, A., Davignon, D., Ku, J.Y., Lohmann, K., Myers, T.C., Park, R.J., Seigneur, C., Selin, N.E., Sistla, G., Vijayaraghavan, K., (2009). An analysis of simulated wet deposition of mercury from the North American Mercury Model Intercomparison Study. Journal of Geophysical Research Atmospheres. 14, D08301.

Byun, D.W., Ching, J.K.S., (1999). Science Algorithms of the EPA Models-3 Community Multiscale Air Quality (CMAQ) Modeling System. EPA-600/R-99/030, US Environmental Protection Agency, US Government Printing Office, Washington, DC.

Calvert J.G., Lindberg S.E., (2005). Mechanisms of mercury removal by O3 and OH in the atmosphere. Atmos Environ 39, 3355–67.

CCC, (2013). Online resource: http://www.nilu.no/projects/ccc/index.html accessed on: May 2013.

Dennis, R., Fox, T., Fuentes, M., Gilliland, A., Hanna, S., Hogrefe, C., Irwin, J., Rao, S.T., Scheffe, R., Schere, K., Steyn, D., Venkatram, A., (2010). A framework for evaluationg regional-scale numerical photochemical modeling system. Environ Fluid Mech (Dordr) 10, 4, 471-489. doi:10.1007/s10652-009-9163-2.

NEN-EN 15853 (en), (2010). Ambient air quality - Standard method for the determination of mercury deposition. ICS 13.040.20, June 2010.

ECE (Economic Commission for Europe), Pirrone, N., Keating, T. (Editors), (2010). Hemispheric Transport of Air Pollution. Part- B: Mercury, United Nations, New York and Geneva.

Gay, D.A., Schmeltz, D., Prestbo, E., Olson, M. Sharac, T. and Tordon, R, (2013). The Atmospheric Mercury Network: measurement and initial examination of an ongoing atmospheric mercury record across North America. ACPD 13, 10521-10546.

Granier, C.; Lamarque, J.; Mieville, A.; Muller, J.; Olivier, J.; Orlando, J.; Peters, J.; Petron, G.; Tyndall, G. & Wallens, S. (2005), 'POET, a database of surface emissions of ozone precursors', http://www.aero.jussieu.fr/projet/ACCENT/POET.php

Haylock, M.R., N. Hofstra, A.M.G. Klein Tank, E.J. Klok, P.D. Jones, M. New. (2008). A European daily high-resolution gridded dataset of surface temperature and precipitation JGR

Houyoux, M. R., Vukovich, J. M., Coats Jr., C. J., et. al., (2000). Emission inventory development and processing for the I-31 Seasonal Model for Regional Air Quality (SMRAQ) project. Journal of Geophysical Research. v105 iD7, 9079-9090, 2000.

Jung, G.; Hedgecock, I. & Pirrone, N. (2009), 'ECHMERIT V1.0 - a new global fully coupled mercury-chemistry and transport model', Geoscientific Model Development **2**, 175-195.

Kerkweg, A.; Buchholz, J.; Ganzeveld, L.; Pozzer, A.; Tost, H. & Jцckel, P. (2006), 'Technical Note: An implementation of the dry removal processes DRY DEPosition and SEDImentation in the Modular Earth Submodel System (MESSy)', Atmospheric Chemistry and Physics **6**(12), 4617—4632.

Kos, G., Ryzhkov, A., Dastoor, A., Narayan, J., Steffen, A., Ariya, P.A., Zhang, L., (2013). Evaluation of discrepancy between measured and modelled oxidized mercury species. Atmos. Chem. Phys. 13, 4839-4863.

Kuss, J., Schneider, B. (2007), Variability of the Gaseous Elemental Mercury Sea-Air Flux of the Baltic Sea. Environ. Sci. Technol. 41, 8018-8023.

Kvietkus K., (1995), Investigation of the gaseous and particulate mercury concentrations along horizontal and vertical profiles in the lower troposphere. In: Anttila, P., Kämäri, J., Tolvanen, M. (Eds.), Proceedings of the 10th World Clean Air Congress. Espoo, Finland, May 28–June 2, p. 284.

Lohman, K., Seigneur, C., Edgerton, E., and Jansen, J., (2006), Modeling mercury in power plant plumes, Environ. Sci. Technol., 40, 3848-3854.

Matthias, V., (2008). The aerosol distribution in Europe derived with the Community Multiscale Air Quality (CMAQ) model: comparison to near surface in situ and sunphotometer measurements (2008). Atmos. Chem. Phys. 8, 5077–5097, www.atmos-chem-phys.net/8/5077/2008/.

Michalakes, J., J. Dudhia, D. Gill, T. Henderson, J. Klemp, W. Skamarock, and W. Wang, (2004). "The Weather Reseach and Forecast Model: Software Architecture and Performance," to appear in proceedings of the 11th ECMWF Workshop on the Use of High Performance Computing In Meteorology, 25-29 October 2004, Reading U.K. Ed. George Mozdzynski.

Pacyna, E. G.; Pacyna, J. M.; Steenhuisen, F. & Wilson, S. (2006), 'Global anthropogenic mercury emission inventory for 2000', Atmospheric Environment 40(22), 4048 – 4063.

Passant, N.R, (2002). Speciation of UK emissions of non-methane volatile organic compunds. AEA Technology Report AEAT/ENV/R/0540 Issue 1, Culham, UK.

Peters, J. A. H. W. & Olivier, J. G. J. (2003), 'EDGAR3/POET Enussuibs; 1997 emissions and scenarios for 1995–2020; Technical background infromation on global and regional sectoral emissions', RIVM, Bilthoven, report no. 773301003.

Rockel, B., Will, A., and Hense, A., (2008). The Regional Climate Model COSMO-CLM (CCLM). Meteorol. Z. 17, 347–248.

Rockel, B. and Geyer, B., (2008). The performance of the regional climate model CLM in different climate regions, based on the example of precipitation. Meteorologische Zeitschrift Band 17, Heft 4, 487– 498.

Roeckner, E.; Вдuml, G.; Bonaventura, L.; Brokopf, R.; Esch, M.; Giorgetta, M.; Hagemann, S.; Kirchner, I.; Kornblueh, L.; Manzini, E.; Rhodin, A.; Schlese, U.; Schulzweida, U. & A., T. (2003), 'The atmospheric general circulation model ECHAM 5. PART I: Model description', Technical report, Max Planck Institute for Meteorology (MPI-M), Hamburg, Germany, MPI-Report No. 349.

Roeckner, E.; Brokopf, R.; Esch, M.; Giorgetta, M.; Hagemann, S.; Kornblueh, L.; Manzini, E.; Schlese, U. & Schulzweida, U. (2006), 'Sensitivity of Simulated Climate to Horizontal and Vertical Resolution in the ECHAM5 Atmosphere Model', J. Climate 19(16), 3771—3791.

Ryaboshapko, A, Bullock R.O., Christensen, J., Cohen, M., Dastoor, A., Ilyin, I., Petersen, G., Syrakov, D., Travnikov, O., Artz, R.S., Davignon, D., Draxler, R.R., Munthe, J., Pacyna, J. (2007a). Intercomparison study of atmospheric mercury models: 1. Comparison of models with short term measurements, Science of the Total Environment 376 (2007) 228–240

Ryaboshapko, A, Bullock R.O., Christensen, J., Cohen, M., Dastoor, A., Ilyin, I., Petersen, G., Syrakov, D., Travnikov, O., Artz, R.S., Davignon, D., Draxler, R.R., Munthe, J., Pacyna, J. (2007b). Intercomparison study of atmospheric mercury models: 2. Modelling results vs. long-term observations and comparison of country deposition budgets , Science of the Total Environment 377 (2007) 319 – 333

Ryaboshapko, A, Bullock R.O., Christensen, J., Cohen, M., Dastoor, A., Ilyin, I., Petersen, G., Syrakov, D., Travnikov, O., Artz, R.S., Davignon, D., Draxler, R.R., Munthe, J., Pacyna, J. (2007c). Intercomparison study of numerical models for Long-Range transport of mercury: Stage 3: Comparison of modelled results with long-term observations and comparison of calculated items of regional balances, EMEP/MSC-E Technical Report 1/2005, Moscow, 2005.

Swartzendruber, P.C., Chand, D., Jaffe, D.A., Smith, J., Reidmiller, D., Gratz, L., Keeler, J., Strode, S., Jaegle, L., Talbot, R., (2008). Vertical distribution of mercury, CO, ozone, and aerosol scattering coefficient in the Pacific Northwest during the spring 2006 INTEX-B campaign. Journal of Geophysical Research 113, D10305. doi:10.1029/2007JD009579

Sander, R.; Kerkweg, A.; Jцckel, P. & Lelieveld, J. (2005), 'Technical note: The new comprehensive atmospheric chemistry module MECCA', Atmospheric Chemistry and Physics 5(2), 445—450.

Strode, S.A., Jaegle, L., Selin, N.E., Jacob, D.J., Park, R.J., Yantosca, R.M., Mason, R.P., Slemr, F., (2007). Air-sea exchange in the global mercury cycle. Global Biogeochem. Cycles 21, GB1017.

Skamarock WC, Klemp JB, Dudhia J, Gill DO, Barker DM, Duda MG, Huang WX-Y Wang, Powers JG (2008) A Description of the Advanced Research WRF Version 3. Tech. rep., National Center for Atmospheric Research

Travnikov, O., and I. Ilyin (2009), The EMEP/MSC-E mercury modeling system, in Mercury Fate and Transport in the Global Atmosphere, edited by N. Pirrone and R. P. Mason, pp. 571-587, Springer, Dordecht.

UNC Carolina Environmental Program, (2005). Sparse Matrix Operator Kernel Emissions (SMOKE) Modeling System, UNC Chapel Hill, North Carolina, USA.

UNEP (United Nations Environment Programme), (2002). Global Mercury Assessment, UNEP, Geneva, Switzerland.

UNEP (United Nations Environment Programme), (2008). Global Atmospheric Mercury Assessmet: Sources, Emissions and Transport, UNEP, Geneva, Switzerland.

UNEP (United Nations Environment Programme), (2013a). Global Mercury Report, UNEP, Geneva, Switzerland, 2013.

UNEP (United Nations Environment Programme), (2013b). Mercury: Time to act. Tech. rep., Chemicals Branch, Division of Technology, Industry and Economics, United Nations Environment Programme (UNEP)

Vijayaraghavan, K., Karamchandani, P., Seigneur, C., Balmori, R., and Chen, S.-Y.: Plume-in-grid modeling of atmospheric mercury, J. Geophys. Res., 113, D24305, doi:10.1029/2008jd010580, 2008.

Weigelt, A., Temme, C., Bieber, E., Schwerin, A., Schuetz, M., Ebinghaus, R., Kock, H.H., (2013). Measurements of atmospheric mercury species at a German rural background site from 2009 to 2011 – methods and results. Environ. Chem., available online: http://dx.doi.org/10.1071/EN12107

Yarwood, G., Rao, S., Yocke, M., Whitten, G.Z., (2005). Updates to the carbon bond chemical mechanism: CB05. Final Report RT-04-00675. Yocke and Company 415.899.0703, Novato, California.

Zager, D.A., Rajar, R., Petovsek, G., Cetina, M., Horvat, M. (2007). Modelling of mercury cycling in the Mediterranean Sea. Rapp. Comm. Int. Mer Médit 28

Zhang, L., Blanchard, P., Gay, D.A., Presbo, E.M., Risch, M.R., Johnson, D., Narayan, J., Zsolway, R., Holsen, T.M., Miller, E.K., Castro, M.S., Graydon, J.A., St. Louis, V.L., Dalziel, J., (2012a). Estimation of speciated and total mercury dry deposition at monitoring locations in eastern and central North America. ACP 12, 4327-4340.

Zhang, L., Blanchard, P., Johnson ,D., Dastoor, A., Tyzhkov, A., Lin, C.J., Vijayaraghavan K., Gay, D., Holsen, T.M., Huang, J., Graydon, J.A., St Louis, V.L., Castro, M.S., Miller, E.K., Marisk, F., Lu, J., Poissant, L., Pilote, M., Zhang, K.M., (2012b). Assessment of modeled mercury dry deposition over the Great Lakes region.

Zhang Y., Jaeglé, L., van Donkelaar, A., Martin, R.V., Holmes, C.D., Amos, H.M., Wang, Q., Talbot, R. Artz, R., Brooks, S., Luke, W., Holsen, T.M., Felton, D., Miller, E.K., Perry, K.D., Schmeltz, D., Steffen, A., Tordon, R., Weiss-Penzias, P., Zsolway. R., (2012c). Nested-grid simulation of mercury over North America. Atmos. Chem. Phys. 2012, 12: 6095-6111.

Figures

Figure 1: Hourly modelled (blue) concentrations compared to 2-hour measurements (red) of atmospheric GOM and PBM at Waldhof for 2009 (Weigelt et al., 2013). Model values shown are from the CMAQ-Hg default model run.

Figure 2: Annual total precipitation (boxes) and deposition (points) for 18 EMEP stations. Observations are based on monthly values obtained by wet deposition samplers for the year 2009. Comparison of observed precipitation and deposition to results from CMAQ-Hg using two different meteorological datasets (CCLM and WRF). The precipitation is represented by colored boxes (red=observation, green=CCLM based model run, blue=WRF based model run) in mm per annum (left y-axis). The deposition is given by points in µg/m² (right y-axis).

Figure 3: Precipitation at Waldhof (DE02) monthly and weekly values from the wet-only deposition sampler and daily values from a co-located Eigenbrodt precipitation sampler (left y-axis in mm) compared to precipitation from CCLM and WRF model results. Moreover, the monthly and weekly deposition is given as points (circles=observation, triangles=CCLM based CMAQ-Hg run, diamonds=WRF based CMAQ-Hg run) in µg/m² on the right y-axis.

Figure 4: Comparison of the frequency distribution of precipitation events from daily observations at Waldhof from an Eigenbrodt sampler (red) to CCLM (green) and WRF (blue) model results. The left y-axis illustrates the number of dry days, given by the super positioned boxes at x=0. The right y-axis gives the number of wet days depicted by histograms for logarithmic precipitation amount bins from 0.1 to 42.5 mm per day. It can be seen, that the models are generally underestimating the amount of days with less than 0.4 mm of precipitation. CCLM underestimates the days with 3 to 12 mm. WRF underestimates the number of dry days.

Figure 5: Detailled analysis of March, April, and May at EMEP station Waldhof. Given are monthly and weekly values from the wet-only deposition sampler and daily values from a co-located Eigenbrodt precipitation sampler (left y-axis in mm) compared to precipitation from CCLM and WRF model results. Moreover, the monthly deposition is given as points (circles=observation, triangles=CCLM based CMAQ-Hg run, diamonds=WRF based CMAQ-Hg run) in µg/m² on the right y-axis.

Figure 6: Mean Normalized Bias for precipitation (blue), deposition flux (red), and mercury concentration in rain water (green) for 18 EMEP stations in 2009. The grey interval indicates the range in which model and observation differ by less than a factor of 2. Values are based on monthly observations and ensembles of CMAQ-Hg using CCLM and WRF meteorology. Figure 6a) depicts biases for the default setup and 6b) for the low GOM CMAQ-Hg setup.

Figure 7: CMAQ-Hg results for GEM dry deposition, TOM dry deposition, GOM wet deposition, PBM wet deposition, and total mercury deposition in µg/m² for summer (top) and winter (bottom). Dry deposition of GEM is set to zero over water bodies to include re-emission from the ocean. Data is based on the low GOM CMAQ-Hg run using CCLM meteorological fields. The total modelled mercury deposition over Europe is 1-5 µg/m² in winter and 5-20 µg/m² in summer.

Figure 8: Relative difference [µg/µg] between the CMAQ-Hg default and low GOM runs for GEM dry deposition, TOM dry deposition, GOM wet deposition, PBM wet deposition, and total mercury deposition in µg/m² for summer (top) and winter (bottom). Data is based on the low GOM/default CMAQ-Hg runs using CCLM meteorological fields.

Figure 9: Relationship of atmospheric concentration (x-axis), precipitation (y-axis), and deposition flux (c-axis). The shaded area indicates the range in which the combined bias of precipitation and concentration is in the range of a factor of 2. The bias of the deposition flux is given by the color table, with green values indicating that the modelled values lie inside a factor of 2 to observations. The lines at x=1 and y=1 separate the plot into four sectors which indicate whether concentration and precipitation are over- or underestimated. The four plots depict CMAQ-Hg results at the Waldhof station (DE02) for different CMAQ runs: a) CLM, b) WRF, c) CLM low GOM, d) WRF low GOM. The runs named 'low GOM' are based on a CMAQ run without primary emissions of GOM and without any PBM from chemical reactions. The observations (C = 11.2 pg/m³, P = 638 mm, D = 4.7 µg/m²) are based on weekly average values.

(Supplementary)
Figure S1: Comparison of monthly CCLM precipitation fields with observations
Figure S2: Comparison of monthly WRF precipitation fields with observation

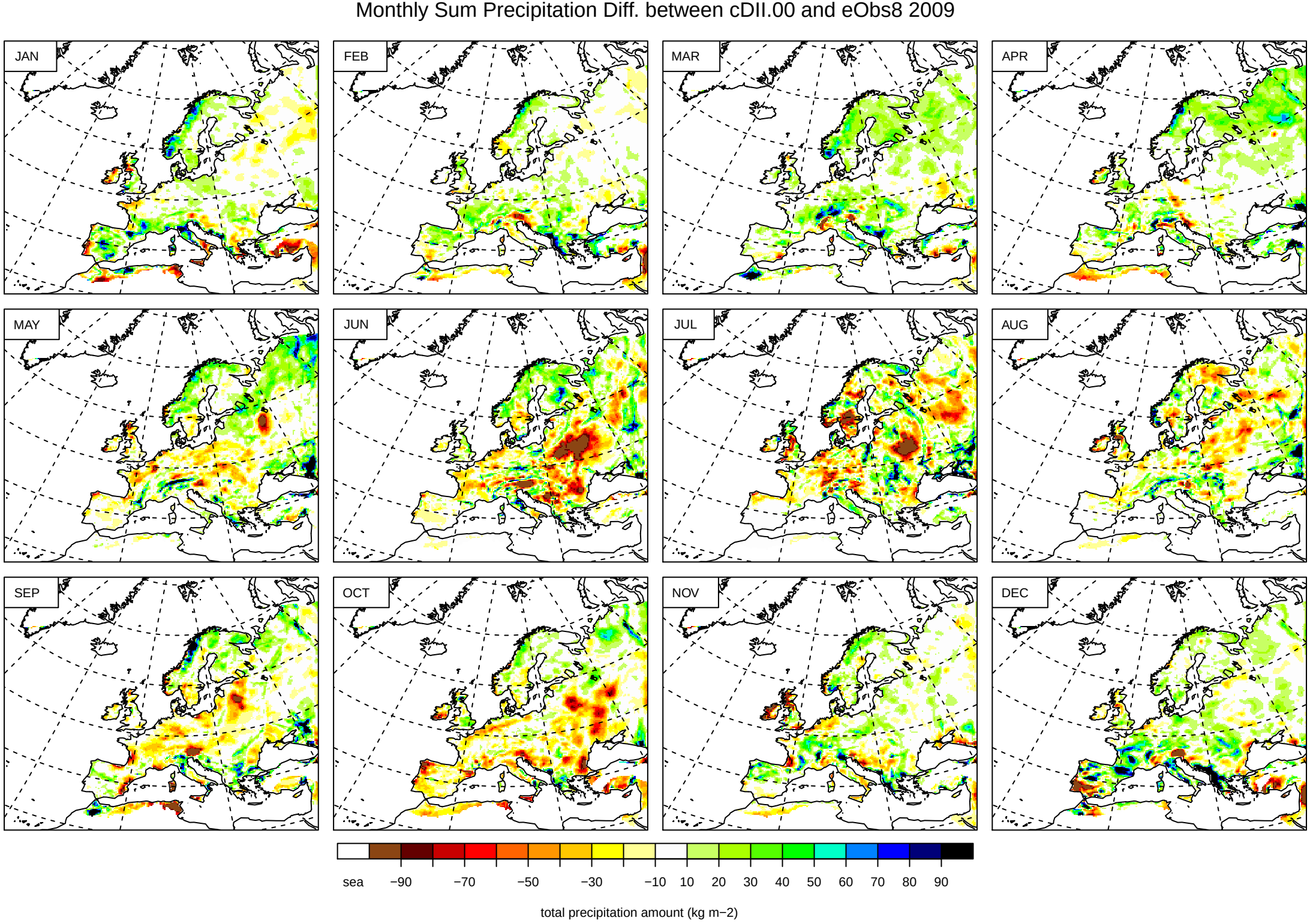
Monthly Sum Precipitation Diff. between cDII.00 and eObs8 2009
JAN
FEB
MAR
APR
MAY
JUN
JUL
AUG
SEP
OCT
NOV
DEC
sea
−90
−70
−50
−30
−10
10
20
30
40
50
60
70
80
90
total precipitation amount (kg m−2)

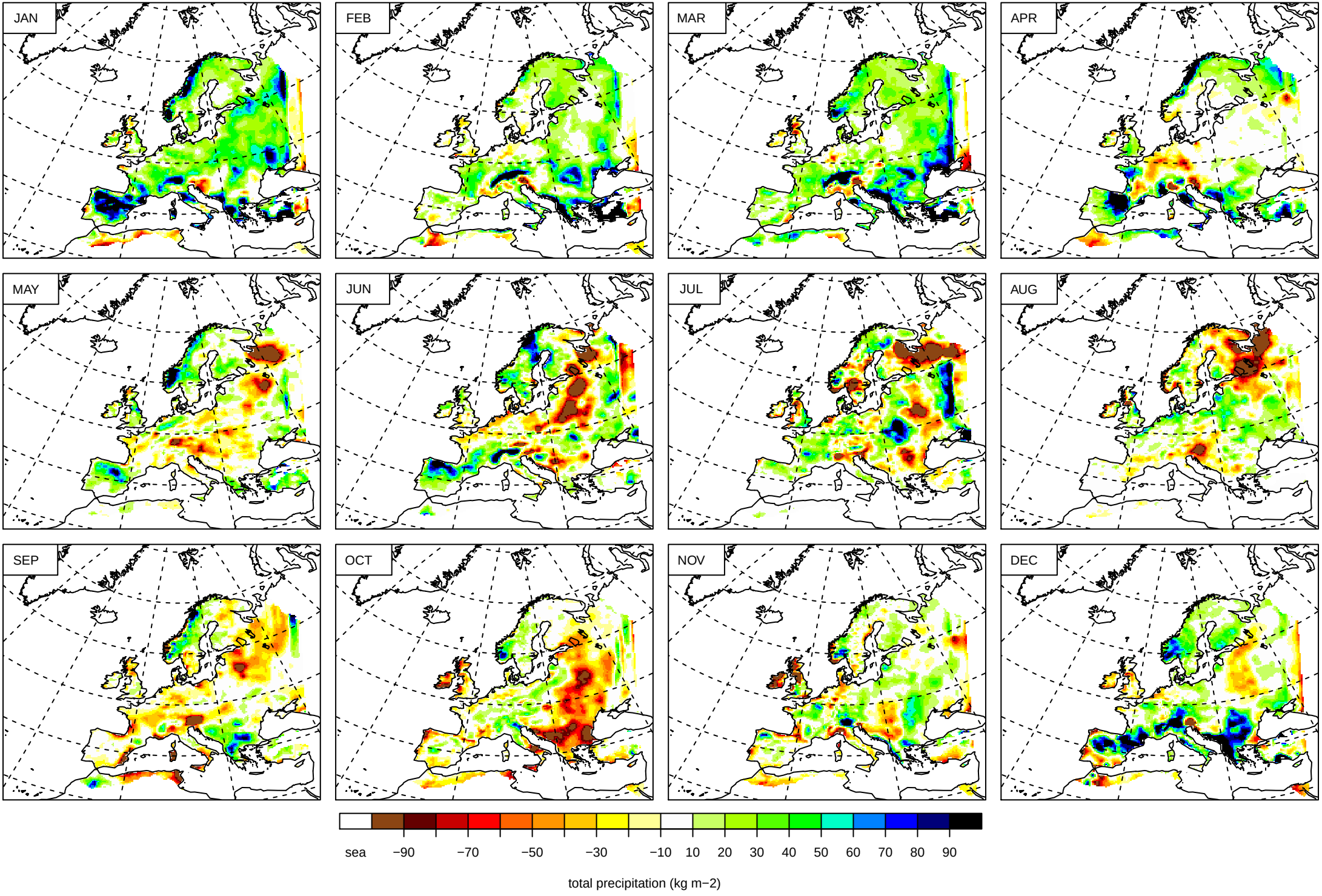
Monthly Sum Precipitation Diff. between wrfout_d01 and eObs8 2009
JAN
FEB
MAR
APR
MAY
JUN
JUL
AUG
SEP
OCT
NOV
DEC
sea
−90
−70
−50
−30
−10
10
20
30
40
50
60
70
80
90
total precipitation (kg m−2)